Transport of cytoskeletal elements in the squid giant axon

MARK TERASAKI*†‡, ALEXANDRA SCHMIDEK*†, JAMES A. GALBRAITH†§, PAUL E. GALLANT*†,
AND THOMAS S. REESE*†

*Laboratory of Neurobiology, National Institute of Neurological Disorders and Stroke, National Institutes of Health, Bethesda, MD 20892-4062; †Marine Biological Laboratories, Woods Hole, MA 02543; and §Department of Bioengineering, University of California at San Diego, La Jolla, CA 92093

ABSTRACT   In order to explore how cytoskeletal proteins are moved by axonal transport, we injected fluorescent microtubules and actin filaments as well as exogenous particulates into squid giant axons and observed their movements by confocal microscopy. The squid giant axon is large enough to allow even cytoskeletal assemblies to be injected without damaging the axon or its transport mechanisms. Negatively charged, 10- to 500-nm beads and large dextrans moved down the axon, whereas small (70 kDa) dextrans diffused in all directions and 1000-nm beads did not move. Only particles with negative charge were transported. Microtubules and actin filaments, which have net negative charges, made saltatory movements down the axon, resulting in a net rate approximating that previously shown for slow transport of cytoskeletal elements. The present observations suggest that particle size and charge determine which materials are transported down the axon.

Transport of cytoskeletal proteins in neurons is thought to be exclusively away from the cell body, toward the terminals of the axon (in the anterograde direction), and is generally referred to as slow axonal transport (1). The rates and polypeptide composition of slow axonal transport have been extensively characterized by following the movement of radiolabeled protein down an axon after injection of precursors into the cell body regions. How cytoskeletal and a variety of other proteins are moved down the axon is unknown, however (1–3). One of the major limitations in formulating a hypothesis about the possible mechanisms and motors responsible for the slow transport of cytoskeletal proteins has been the unavailability of an *in vitro* system in which to study cytoskeletal protein transport (3–5). In this paper we describe the transport of injected cytoskeletal proteins and other negatively charged polymers into the squid giant axon *in vitro*. This system may provide a model in which slow transport can be studied.

MATERIALS AND METHODS

Squids (*Loligo pealeii*) were obtained through the Marine Resources Center at the Marine Biological Laboratory (Woods Hole, MA). The hindmost stellar nerve, or giant axon (380–450 μm diameter), was dissected under running sea water, and all small adherent nerve fibers and loose connective tissue were removed. Damage due to dissection was assessed with darkfield illumination, since localized white spots can be seen where calcium enters large wounds (6, 7), and swollen vesicles or disorganized axoplasm are readily apparent. Axons with such signs of damage were discarded.

Mercury pipettes, which allow greater control by damping of the applied pressure (8), were used to make quantitative injections. Injection pipettes were back-filled with a droplet of mercury, the tip was broken to a diameter of 2–3 μm, and the mercury was advanced to the tip by pressure. The pipette was then front-loaded with the fluorescent injectate, followed by an oil cap (Wesson soybean oil) which prevented both the loss of injectate and contamination of the injectate with seawater. The injection pipette was held parallel to the stage of an upright Zeiss Axioskop with a Narashige (Tokyo) SM-20 manipulator. Although a significant force was required to penetrate the 20- to 30-μm-thick connective tissue sheath, the axon was not damaged during the insertion or the microinjection process as assessed by the absence of localized whitening. Pressure for the injection was applied with a Gilmont (Great Neck, NY) S-1200 syringe filled with Fluorinert (FC-70; Sigma) to transmit the pressure. The microscope was coupled to a laser scanning confocal microscope (model 600; Bio-Rad). A plan-neofluor ×10 0.3-n.a. objective lens was used for the injections, a plan-neofluor ×20 0.5-n.a. lens was used for air observations, and a plan-neofluor ×40 1.3-n.a. lens was used for oil-immersion observations. The injection was observed by simultaneous transmitted light and fluorescence in continuous scanning mode and was recorded on an optical memory disk recorder (Panasonic TQ-3038F). Time sequence images were stored on the computer hard disk.

The injection chamber was constructed by using a strip of silicone rubber sheet (Ronsil, 0.76 mm thick; North American Reiss, Blackstone, VA) as the rear wall with a cantilevered coverslip as the top, and the chamber was filled with natural seawater. For oil-immersion observations, a separate chamber was constructed by applying parallel strips of double-stick tape to a glass slide to form a channel whose height approximated the diameter of the axon. The injected axon was then manipulated so that the oil drop which marked the injection site was on top. The chamber was filled with natural seawater, a coverslip was placed on top of the axon, and the chamber was sealed with silicone grease.

For the experiments on movement of injected oil drops alone, axons were dissected and maintained in an internal buffer (6). The exterior was coated with carbon-black particles prepared by grinding activated charcoal into 1- to 10-μm particles. The inert oil (Fomblin fluorocarbon; Fomblin Industries, Tokyo) was pressure injected under a Zeiss dissecting microscope by use of a micropipette. Other experiments with oil drops were done with *in situ* preparations of *Loliguncula brevis* (shipped live from Galveston, TX). The mantle was opened and bathed with seawater. Carbon black was sprinkled on the top and bottom of the axon to control for curvature changes in the *in situ* axons during the 3-hr experiments, and the axon was pressure injected with oil.

All fluorescent molecules were obtained from Molecular Probes and were dissolved in an injection buffer (100 mM potassium glutamate/10 mM Hepes, pH 7). Approximately 600 pl was injected. The beads used (Latex FluoSpheres) were carboxylate-modified (negatively charged), 100–1000 nm in diameter, with yellow-green fluorescence (490 nm/515 nm) and amidine-modified (positively charged), 200 nm in diameter, with red fluorescence (580 nm/605 nm). A 1:10 dilution of

‡Present address: Department of Physiology, University of Connecticut Health Center, Farmington, CT 06032.

the beads was injected into the axon. The fluorescent dextrans injected were 400-kDa Ficoll (10 mg/ml), 70 kDa or 5- to 40-MDa fluorescein-dextran (2.5 mg/ml, centrifuged at 2000 × g for 5 min), and 500-kDa rhodamine-dextran (5 mg/ml). The charge on the fluorescein-dextrans was 3–8 for the 70-kDa dextran, 13–130 for the 500-kDa dextran, and >100 for the 5- to 40-MDa dextran.

Rhodamine-conjugated (succinimidyl ester linkage) bovine brain tubulin was obtained from Molecular Probes. Eight microliters of 10 mg/ml stock solution was added to 9 μl of internal buffer (6) with 20 μM paclitaxel (former generic name, taxol) for 30–60 min. The polymerized microtubules were triturated 20 times to get smaller microtubule fragments. The amount injected was 600 pl, which corresponds to 0.5 ng. Lyophilized rabbit muscle actin was a gift from D. Fishkind (University of Notre Dame, South Bend, IN). Rhodamine-phalloidin-labeled actin filaments were made essentially as described (9). Actin filaments (1 mg) were assembled in 75 mM KCl/2 mM MgCl$_2$/2 mM Tris acetate, pH 7/0.1 mM ATP/ 0.125 mM dithiothreitol by incubation at 22°C for 1 hr and then were labeled with 6.6 μM rhodamine-phalloidin in assembly buffer with ATP and dithiothreitol for 45 min on ice. To assess the polymerization and labeling, the actin was observed by fluorescence microscopy before the injection. The concentration of injected actin was 4.2 μM and the amount injected was 0.1 ng.

RESULTS

One possible mechanism for slow transport is that the whole axoplasm or large, tightly associated cytoskeletal networks are transported down the squid giant axon. To test this possibility, oil drops (fluorocarbon; 10–20 μm in diameter) were injected into the axoplasm of isolated axons from the squid *Loligo pealeii*. The oil drops did not move relative to carbon-black particles placed on the connective tissue sheath of the axon to serve as stationary reference points. Three hours after injection, there was essentially no movement of the oil drop in relation to the carbon-black markers (≤0.010 ± 0.072 mm/day in the anterograde direction; mean ± SD, n = 10), while video-enhanced differential interference contrast microscopy confirmed that fast axonal transport continued in the axon at this time. In other experiments, oil drops injected into axons maintained intact in the mantle of *Loliguncula brevis* made no net movement relative to carbon markers in the sheath (0.048 ± 0.120 mm/day, retrograde direction, n = 9). If the axoplasmic cytoskeleton were moving down the axon, oil droplets would presumably have moved with it.

Another possible mechanism of slow transport is that small particles or assemblies of polymerized axoplasmic materials individually move down the axon. Negatively charged beads are known to move in the anterograde direction when injected into crab axons (10). To see whether cytoskeletal elements could also move in this manner, we injected fluorescent microtubules and actin filaments into the squid giant axon, directly observing injections as well as subsequent movements by confocal microscopy (Fig. 1*A*). The oil cap in the microinjection pipette formed a spherical drop after being injected, marking the injection site. Since oil droplets remain stationary in the axoplasm, the oil cap provided a fixed reference marker to gauge movement of the fluorescent particulates. A wide range of fluorescent beads with various diameters and surface charges were also injected in order to establish the criteria governing transport of particulate materials in the squid axon.

Negatively charged beads 10 nm, 20 nm, 200 nm, and 500 nm in diameter moved in the anterograde direction, but negatively charged 1000-nm beads and positively charged 10-nm beads did not move. Movements of individual beads resolved by high-numerical-aperture optics were documented in images taken every 15 sec (Fig. 2*A*). The beads appeared to move in
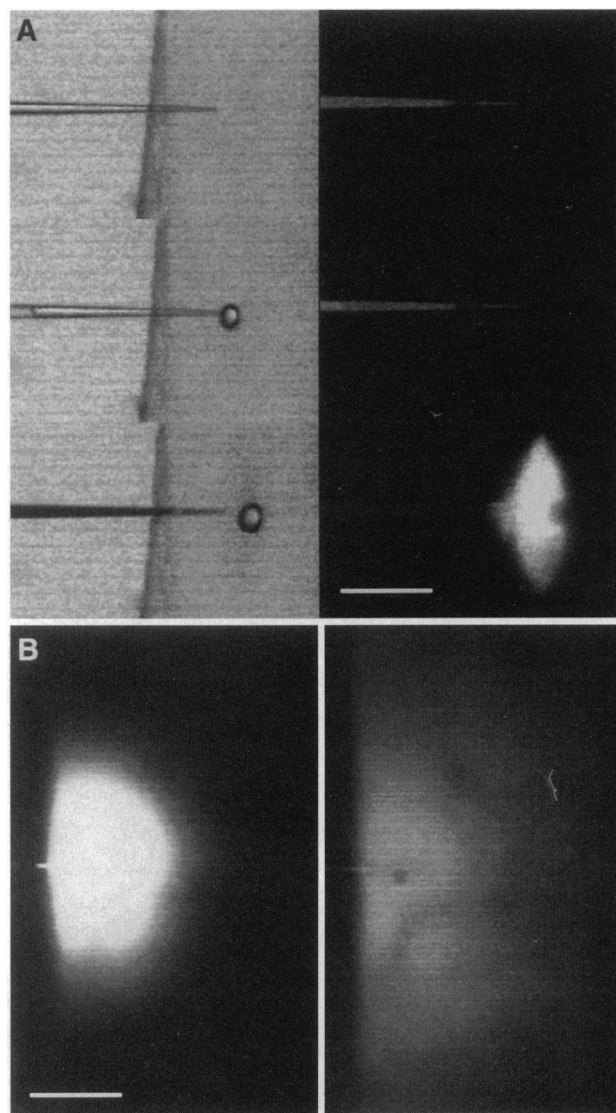

FIG. 1. (*A*) Injection of a fluorescent marker (rhodamine-conjugated 500-kDa dextran) into the squid giant axon. The injection was imaged at 1-sec intervals by simultaneous scanning transmission (*Left*) and fluorescence confocal (*Right*) microscopy. The second image shows the expulsion of the oil cap from the pipette and the third shows expulsion of the dextran. (*B*) Movement of fluorescein-conjugated 70-kDa dextran. The first image was taken ≈1 min after injection, and the second image 19.5 min afterwards. The dextran moved uniformly in all directions (Bars = 50 μm.)

a linear fashion, suggesting that they were moving along filamentous substrates; they could stop and start but showed no sustained reversals of movement. In a region away from the injection site, to which particles were presumably transported after their injection, the positions of every distinguishable particle were followed through 17 intervals. The median rate of anterograde movements was 0.078 μm/sec, and the maximum rate in any interval was 0.4 μm/sec (Fig. 2*D*). The estimated net rate of the whole population of beads, obtained by taking into account all displacements including pauses, was 0.023 μm/sec, or 2.0 mm/day. The possibility that the beads were binding to moving organelles was considered by examining the tracks distal to the injection sites by electron microscopy. This was possible because the oil droplet could be clearly seen in Araldite-embedded axons after fixation with glutaraldehyde and osmium. No associations between beads and organelles that had been transported from the injection site were found in three axons.
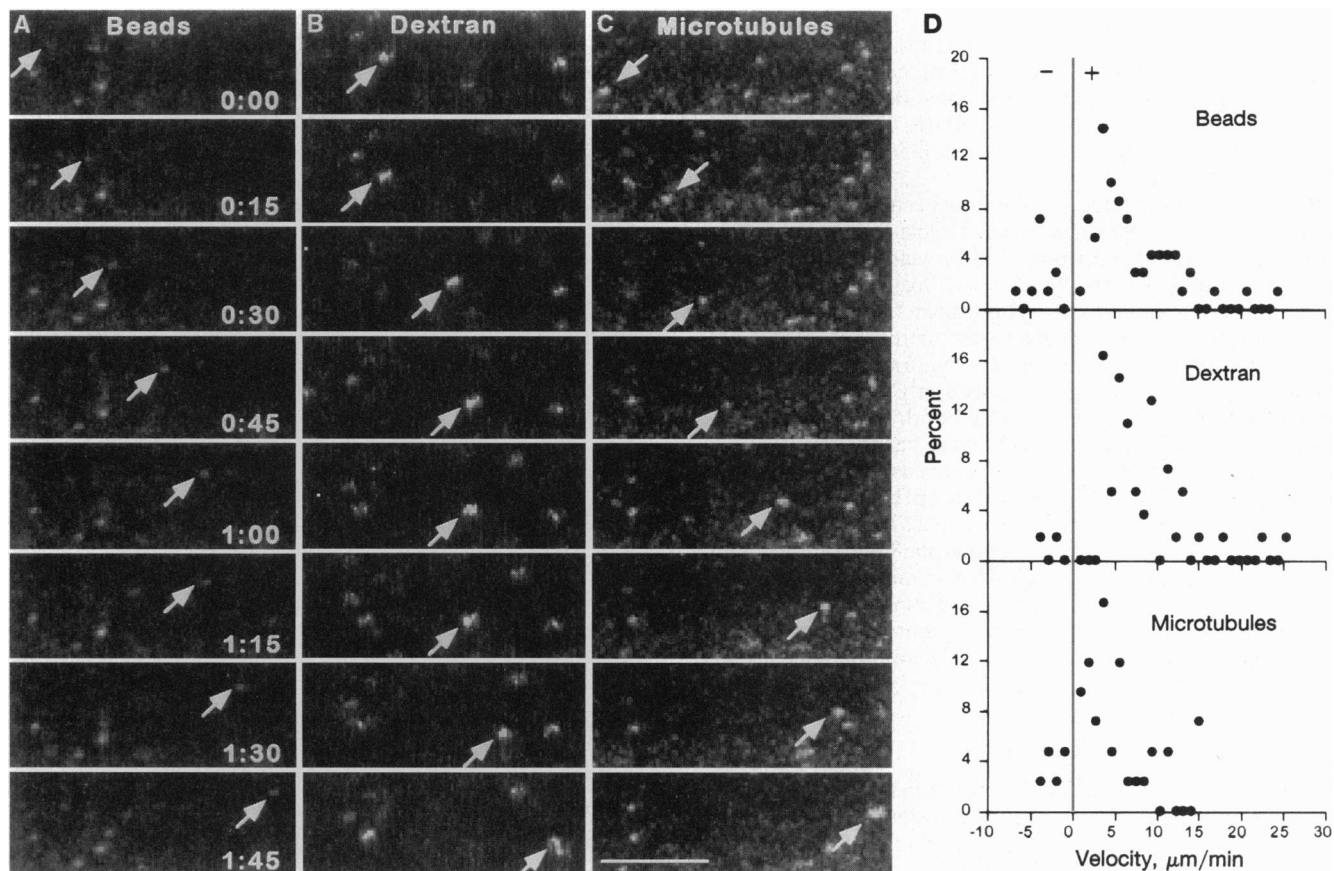
FIG. 2.   Movements of individual injected particulates seen at 15-sec intervals. Arrowheads indicate movement of a 20-nm latex bead (*A*), a 5- to 40-MDa dextran particle (*B*), and a microtubule fragment (1-min pause between the third and fourth frame not shown) (*C*). Movements are predominantly in the anterograde direction. The particles move in a saltatory fashion. (Bar = 10 μm.) (*D*) Apparent instantaneous velocities. For the beads the analyzed sequence lasted 4.25 min (17 frame intervals). The data was collected by determining the displacements of all particles between successive frames. There were 70 moves and 215 pauses (i.e., between any successive frames, an average of 25% of the particles moved and 75% were stationary). For the dextran the sequence was 3.25 min. There were 55 moves and 288 pauses. For the microtubule fragments (<10%) there were fewer moves, so a different approach was used. In a 14.5-min sequence, 6 fragments that were visible for more than 6 frames were followed. There were 42 moves and 59 pauses.

Since carboxylated latex beads have been shown to move anterogradely when exposed to purified kinesin (11), we tested the possibility that the fluorescently labeled beads bound kinesin directly. Immunostained Western blots demonstrated that 20 μl of packed beads bound most of the kinesin present in ≈20 μl of axoplasmic supernatant diluted into 5 volumes of axoplasmic buffer (11), but the beads bound very little tubulin, actin, or other major proteins present in the axoplasmic supernatant. Kinesin thus appears to have a high affinity for the carboxylated latex beads used for injections.

The charge of fluorescently labeled dextrans and Ficolls (inert polysaccharides) is largely determined by the fluorophore—fluorescein conjugates are negative whereas rhodamine conjugates are neutral (12). Negatively charged, fluorescein-conjugated molecules of high molecular mass (5- to 40-MDa dextran and 400-kDa Ficoll) moved anterogradely, as indicated by the emergence of a visible plume of material in the anterograde direction away from the injection site as well as by movements of individual particles seen with high-numerical-aperture optics (Fig. 2*B*). The median rate of anterograde movement was 0.11 μm/sec, and the maximum rate was 0.43 μm/sec (Fig. 2*D*). The estimated net rate of movement of the population of dextran particles was 0.02 μm/sec, or 1.7 mm/day. A small fluorescent dextran (70 kDa, fluorescein-conjugated, net negative charge) appeared to diffuse uniformly in all directions (Fig. 1*B*). A neutrally charged, rhodamine-conjugated 500-kDa dextran also diffused in all directions.
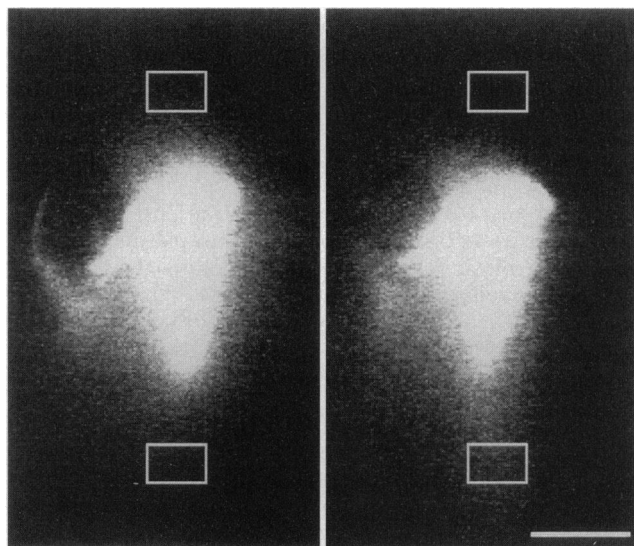

FIG. 3.   Movement of rhodamine-phalloidin-labeled actin filaments seen with low-numerical-aperture optics. The left image was taken ≈1 min after the injection, and the right image was obtained 44 min 30 sec later. The fluorescence has moved away from the injection site in the anterograde direction (downwards). To document this movement, measurements were made within the white rectangles; the area within the white lines is 15.6 μm × 10 μm. The average intensities within the regions are as follows: upper left, 10.8; upper right, 8.3; lower left, 10.3; lower right, 14.8; black = 0, white = 255. (Bar = 25 μm.)

Table 1.   Movements of various injectates in squid giant axon

Diffused in all directions	Moved anterogradely	Did not move
70-kDa Fl-dextran (−)	5- to 40-MDa Fl-dextran (−)	1000-nm Fl-beads (−)
500-kDa Rh-dextran (neut)	400-kDa Fl-Ficoll (−)	20-nm Rh-beads (+)
	10- to 500-nm Fl-beads (−)	Oils (fluorocarbon, soybean)
	Microtubule fragments (−)	
	Actin filament fragments (−)	

Fl, fluorescein; Rh, rhodamine; −, negatively charged; +, positively charged; neut, neutral.

Fluorescent microtubule fragments were prepared by adding paclitaxel to purified, rhodamine-labeled bovine brain tubulin. The fluorescence from the labeled microtubule fragments moved anterogradely as seen with a low-numerical-aperture lens (data not shown), and individual moving fragments were resolved with the oil-immersion lens (Fig. 2C). However, the fraction of particles moving was less than that seen with the latex beads or dextrans. The median velocity of six particles moving anterogradely was 0.063 μm/sec, and the maximum rate was 0.25 μm/min (Fig. 2C). By averaging in the pauses, the net rate of movement of these particles was calculated to be 0.03 μm/sec, or 2.6 mm/day.

Fluorescent actin filaments were prepared by polymerization of purified muscle actin followed by labeling with rhodamine-phalloidin. At low magnification, the fluorescence moved only in the anterograde direction as confirmed by measuring the fluorescence intensity in the retrograde and anterograde directions (Fig. 3). Even with oil-immersion optics, spots presumably corresponding to actin filaments were difficult to follow, confounding calculation of a rate.

DISCUSSION

Results of all injections are summarized in Table 1. As in crab axons (10), negatively charged latex beads smaller than 500 nm in diameter move anterogradely, whereas positively charged beads do not move. Similarly, negatively charged large dextrans move anterogradely, whereas neutrally charged dextrans and small negatively charged dextrans diffuse in all directions. All the injected particles that move, including the cytoskeletal proteins (13), are negatively charged at the pH of axoplasm, which suggests that any negatively charged axoplasmic particle or protein assembly falling within a wide range of sizes will be transported in the anterograde direction.

All the negatively charged particles that move down the axon have similar maximum velocities, suggesting that they could be moved by the same motor. The large pool of soluble kinesin (11) might provide this motor. The kinesin heavy chain has in its tail a region of positively charged amino acids (14) that is proposed to be the binding site for objects moved by kinesin *in vitro* (15). The tail region binds microtubules (16, 17) and is thought to provide the means for microtubule–microtubule sliding (17). The kinesin tail region could also provide a means to attach kinesin to any particles or protein assemblies with a negative charge.

The maximal rate of the soluble kinesin motor appears to be around 0.5 μm/sec (11, 18); close to the maximal rates of movements of injected beads, dextrans, and microtubule fragments, 0.25–0.43 μm/sec (Fig. 2). The similarity of the maximum velocity of particle movements to the velocity of the soluble kinesin is another reason to suggest that it is the motor for the movements reported here. We cannot exclude the possibility, however, that soluble axoplasmic myosins (19, 20), which move at a velocity similar to that of kinesin (20–22), might also be involved in moving injected particles and cytoskeletal fragments.

The squid giant axon is large enough to allow injection of not only soluble monomers but also large cytoskeletal proteins or

protein assemblies without damaging the axon or its transport mechanism. Observation of these fluorescently labeled proteins has provided a direct method of assessing their movement. While the maximum velocity of the injected particles is severalfold greater than the rates reported for slow transport, the particles we observed typically stop and start rather than move continuously down the axon. Indeed, the resulting slow net rate of movement down the axon (<0.05 μm/sec) is in the range of net rates reported for the slow axonal transport of cytoskeletal proteins (1). Thus, the squid giant axon is a promising model system in which to test some of the proposed mechanisms for slow axonal transport and, more generally, to explore the mechanisms available to transport cytoskeletal proteins.

1.   Grafstein, B. & Forman, D. S. (1980) *Physiol. Rev.* **60,** 1167–1283.
2.   Lasek, R. J. (1986) *J. Cell Sci. Suppl.* **5,** 161–179.
3.   Okabe, S. & Hirokawa, N. (1989) *Curr. Opin. Cell Biol.* **1,** 91–97.
4.   Keith, C. H. (1987) *Science* **235,** 337–339.
5.   Reinsch, S. S., Mitchison, T. J. & Kirschner, M. (1991) *J. Cell Biol.* **115,** 365–379.
6.   Gallant, P. E. (1988) *J. Neurosci.* **8,** 1479–1484.
7.   Gallant, P. E. (1992) *J. Neuropathol. Exp. Neurol.* **51,** 220–230.
8.   Kiehart, D. P. (1982) *Methods Cell Biol.* **25,** 13–31.
9.   Cao, L. G. & Wang, Y. L. (1990) *J. Cell Biol.* **111,** 1905–1911.
10.   Adams, R. J. & Bray, D. (1983) *Nature (London)* **303,** 718–720.
11.   Vale, R. D., Reese, T. S. & Sheetz, M. P. (1985) *Cell* **42,** 39–50.
12.   Haugland, R. P. (1992) *Handbook of Fluorescent Probes and Research Chemicals* (Molecular Probes, Inc., Eugene, OR).
13.   Stebbings, H. & Hunt, C. (1982) *Cell Tissue Res.* **227,** 609–617.
14.   Kosik, K. S., Orecchio, L. D., Schnapp, B., Inouye, H. & Neve, R. L. (1990) *J. Biol. Chem.* **265,** 3278–3283.
15.   Navone, F., Niclas, J., Hom-Booher, N., Sparks, L., Bernstein, H. D., McCaffrey, G. & Vale, R. D. (1992) *J. Cell Biol.* **117,** 1263–1275.
16.   Andrews, S. B., Gallant, P. E., Leapman, R. D., Schnapp, B. J. & Reese, T. S. (1993) *Proc. Natl. Acad. Sci. USA* **90,** 6503–6507.
17.   Urrutia, R., McNiven, M. A., Albanesi, J. P., Murphy, D. B. & Kachar, B. (1991) *Proc. Natl. Acad. Sci. USA* **88,** 6701–6705.
18.   Vale, R. D., Schnapp, B. J., Reese, T. S. & Sheetz, M. P. (1985) *Cell* **40,** 559–569.
19.   Bearer, E. L., DeGiorgis, J. A., Bodner, R. A., Kao, A. W. & Reese, T. S. (1993) *Proc. Natl. Acad. Sci. USA* **90,** 11252–11256.
20.   Langford, G. M., Kuznetsov, S. A., Johnson, D., Cohen, D. L. & Weiss, D. G. (1994) *J. Cell Sci.* **107,** 2291–2298.
21.   Kuznetsov, S. A., Langford, G. M. & Weiss, D. G. (1992) *Nature (London)* **356,** 722–725.
22.   Kuznetsov, S. A., Rivera, D. T., Severin, F. F., Weiss, D. G. & Langford, G. M. (1994) *Cell Motil. Cytoskeleton* **28,** 231–242.